

● *Original Contribution*

ON THE POTENTIAL OF THE LAGRANGIAN ESTIMATOR FOR ENDOVASCULAR ULTRASOUND ELASTOGRAPHY: *IN VIVO* HUMAN CORONARY ARTERY STUDY

ROCH L. MAURICE,* JÉRÉMIE FROMAGEAU,* ÉLISABETH BRUSSEAU,[†] GÉRARD FINET,[‡]
GILLES RIOUFOL,[‡] and GUY CLOUTIER*

*Laboratory of Biorheology and Medical Ultrasonics, Research Center, University of Montreal Hospital, Montreal, Canada; [†]CREATIS, UMR CNRS 5515, affiliated to INSERM, Lyon, France; and [‡]Department of Hemodynamics, Cardiovascular Hospital, Claude Bernard University, Lyon, France

(Received 7 July 2006; revised 12 January 2007; in final form 31 January 2007)

Abstract—Diagnosis and prognosis of coronary artery atherosclerosis evolution currently rely on plaque morphology and vessel stenosis degree. Such information can accurately be assessed with intravascular ultrasound (IVUS) imaging. A severe complication of coronary artery atherosclerosis is thrombosis, a consequence of plaque rupture or fissure, which might lead to myocardial infarction and sudden ischemic death. Plaque rupture is a complicated mechanical process, correlated with the plaque morphology, composition, mechanical properties and with the blood pressure. Extracting information on the plaque local mechanical properties may reveal relevant features about plaque vulnerability. Accordingly, endovascular elastography (EVE) was introduced to complement IVUS for investigating coronary artery diseases. In this article, *in vivo* elastographic data are reported for three patients (patient 1, patient 2 and patient 3) who were diagnosed with severe coronary artery stenoses. Time-sequence radio-frequency (RF) data were acquired, in the minutes preceding angioplasty, using an ultrasound scanner working with a 30 MHz mechanical rotating single-element transducer. The elastograms of the radial strain and radial shear distributions within the vessel wall were computed from pairs of successive RF images using the Lagrangian estimator (LE). A hard atherosclerotic plaque (low radial strain and shear) was identified in patient 1. High radial strain and shear values in the plaque areas for patient 2 and patient 3 suggested the presence of lipid cores (soft materials), known to be prone-to-rupture sites when located close to the lumen. To conclude, EVE allowing radial strain and shear images is an improvement over existing EVE methods that may assist IVUS in preoperative vessel lesion assessments and in endovascular therapy planning. (E-mail: guy.cloutier@umontreal.ca) © 2007 World Federation for Ultrasound in Medicine & Biology.

Key Words: Endovascular elastography, Lagrangian estimator, Vulnerable plaque, Atherosclerosis, Coronary artery diseases, Ultrasound imaging.

INTRODUCTION

Atherosclerosis is characterized by a focal accumulation of lipids, complex carbohydrates, blood cells, fibrous tissues and calcified deposits, forming a plaque that thickens and hardens the arterial wall. A severe complication of atherosclerosis is thrombosis, a consequence of plaque rupture or fissure, which might be fatal according to the event localization (Davies and Thomas 1985; Falk 1989; Naghavi et al. 2003; Zaman et al. 2000). Plaque

rupture is a complicated mechanical process, correlated with plaque morphology, composition, mechanical properties and with the blood pressure and its long term repetitive cycle (Falk 1992; Fung 1993). Owing to that, assessing plaque local mechanical properties may, thus, reveal relevant insights about plaque vulnerability (Fisher et al. 2000; Ohayon et al. 2001). This gave rise to endovascular ultrasound elastography (EVE) that was introduced to complement intravascular ultrasound (IVUS) echograms in the assessment of vessel lesions and for endovascular therapy planning (de Korte et al. 2000).

EVE is a catheter-based modality, which gives insights about mechanical properties of the vessel wall. Mechanical parameters (radial strains and shears, in the current article) are estimated from time-sequences of

Address correspondence to: Dr Guy Cloutier, Director of the Laboratory of Biorheology and Medical Ultrasonics, Research Center, University of Montreal Hospital, 2099 Alexandre de Sève (room Y-1619), Montreal, Quebec, Canada, H2L-2W5. E-mail: guy.cloutier@umontreal.ca

radio-frequency (RF) data acquired from the vascular tissue during the cardiac pulsation. The one-dimensional (1D) correlation-based tissue motion estimator is the commonly used technique to assess motion in EVE (de Korte et al. 2000). However, vascular tissue is heterogeneous and its kinematics is likely very complex and subjected to nonrigid rotation, shear, scaling, etc. To take into account signal decorrelation induced by such complex movements, the Lagrangian estimator (LE) was recently proposed for motion computation in EVE (Maurice et al. 2004a, 2005a). This model-based estimator allows the computation of the full two-dimensional (2D) strain tensor.

On the other hand, the determinants of ruptured plaques are known to be a large lipid core covered by a thin fibrous cap and/or a dense infiltration of macrophages inside the fibrous cap (Davies et al. 1993; Fuster et al. 2005). Interestingly, using Yucatan pig models of atherosclerosis in iliac and femoral arteries, de Korte et al. (2002) showed that EVE was capable of identifying such plaque components. Whereas in those animal models only homogeneous plaque types were documented, human plaques are more complex, being mostly constituted of heterogeneous materials. In the current article, an *in vivo* investigation of EVE on pathologic human subjects is presented. Indeed, elastographic data are reported for three patients who underwent angioplasty examinations. It is worth emphasizing that this is the first time that radial shear elastograms are presented in an *in vivo* study, thanks to the Lagrangian estimator.

MATERIALS AND METHODS

Experimental protocol

IVUS data were acquired during coronary angioplasty. Patients underwent a percutaneous coronary intervention (PCI) after being referred for a first acute coronary syndrome-non ST elevation acute myocardial infarction (ACS-NSTEMI). All interventions were performed within 24 h following the onset of symptoms. When the culprit lesion was clearly identified, the cardiologist made a first selection using angiography to determine which patients were to be considered for a complementary IVUS examination. Typically, those with significant calcified plaques were excluded. IVUS exploration began from the coronary artery contralateral to the artery housing the culprit lesion. All patients provided written informed consent.

Three male patients, labeled patient 1, patient 2 and patient 3, and 53, 77 and 66 y-old, respectively, underwent RF IVUS data acquisitions. The right coronary artery (RCA) was investigated for patient 1, who was a smoker also diagnosed with dyslipidemia and having a left ventricular ejection fraction (LVEF) at 74%. For

patient 2, also diagnosed with diabetes, hypertension and dyslipidemia, the LVEF was 56%. The IVUS recording was performed within the left anterior descending artery (LADA). Patient 3 had documented hypertension and dyslipidemia. His LVEF was 63% and the LADA was scanned with IVUS.

Experimental set-up

The experimental set-up consisted in a CVIS (Clear-View, CardioVascular Imaging System Inc., Sunnyvale, CA, USA) ultrasound scanner, coupled with a 30 MHz mechanical rotating single-element transducer along with an Atlantis SR C4020 catheter (Boston Scientific, Natick, MA, USA). The signals were digitized with an oscilloscope LECROY 9374L (LeCroy Corporation, Chestnut Ridge, NY, USA) and stored in a 500-MB PCMCIA disk. The main advantage of this system was its small size that allowed bringing it easily into the intervention cardiology room. However, the main disadvantage was the small 4-MB memory capacity of the oscilloscope, which was the physical limit of the acquired data length. The number of images digitized during one data record depended on the sampling frequency and on the exploration depth, which differed from patient to patient. The sampling frequency was varied from 200 to 500 MHz. The higher the sampling frequency, the more robust is the strain estimation since there are more samples within a single wavelength. On the other hand, with a 500 MHz sampling frequency, only three images could be recorded per acquisition due to the memory capacity limitation, whereas seven images were recorded at a sampling frequency of 200 MHz.

Patient 2 and patient 3 data were digitized at 200 MHz; this corresponds to 2.9 mm and 6.3 mm depth, 763×256 pixels (5×5 mm²) and 1651×256 pixels (5×5 mm²), respectively. Patient 1 data were digitized at 500 MHz due to the apparent large motion of the coronary artery; this corresponds to 1.6 mm depth and 1041×256 pixels (5×5 mm²) RF images. To implement the LE method outlined below, a measurement-window (MW) of 200 samples on the vertical axis by 20 RF lines on the horizontal axis, with 94% axial and 90% lateral overlaps was used (Maurice et al. 2004b). Because of the resolution discrepancy between the data of patient 1, patient 2 and patient 3, the MWs were $960 \mu\text{m} \times 390 \mu\text{m}$, $1.3 \text{ mm} \times 390 \mu\text{m}$ and $605 \mu\text{m} \times 390 \mu\text{m}$, respectively. No attempt was made to optimize the MWs. On the other hand, all RF data sets were over-sampled by a factor of five with the purpose of improving elastogram resolution. The elastograms were computed off-line from each pair of consecutive RF data and were postprocessed using a 2×2 -kernel Gaussian filter.

The Lagrangian estimator

The Lagrangian estimator, which was used to compute the endovascular elastograms, is described elsewhere (Maurice *et al.* 2004a, 2005a). Assuming small MWs and affine tissue motion between two RF images, it can mathematically be formulated as the following nonlinear minimization problem:

$$\min_{[LT_p]} \|RF(r, \varphi, t) - RF_{Lag}(r, \varphi, t + \delta t)\|^2, \quad (1)$$

where (r, φ) defines the image coordinate system, and “ t ” indicates the time. $RF(r, \varphi, t)$ is the pretissue-motion RF image, and $RF_{Lag}(r, \varphi, t + \delta t)$ is the Lagrangian image (LI) at time “ $t + \delta t$ ” (Maurice *et al.* 2004a). The minimum of eqn 1 was obtained using the appropriate $[LT_p]$, a 2D linear transformation matrix associated with the polar coordinate system (r, φ) . It was demonstrated that $[LT_p]$ is related to the strain tensor ε *via* the following relationship (Maurice *et al.* 2004a):

$$\varepsilon_{ij}(t) = \frac{1}{2}[\Delta_{ij}(t) + \Delta_{ji}(t)]$$

with

$$\Delta = LT_p - I = \begin{bmatrix} \frac{\partial U_\varphi}{\partial \varphi} & \frac{\partial U_\varphi}{\partial r} \\ \frac{\partial U_r}{\partial \varphi} & \frac{\partial U_r}{\partial r} \end{bmatrix}. \quad (2)$$

In this equation, U_r and U_φ are the radial and tangential displacement fields, respectively. Δ is defined as the deformation matrix, with Δ_{rr} ($= \varepsilon_{rr}$) and $\Delta_{r\varphi}$, being the radial strain and radial shear, respectively. The maps of Δ_{rr} and $\Delta_{r\varphi}$ distributions provide the elastograms shown in the current study. $[I]$ is the 2D-identity matrix.

Equation 1 was solved using the optical flow-based implementation of the LE described in Maurice *et al.* (2005b). It is based on the assumption that, for small tissue motions, the RF data contain an “acoustical signature” of displacements of scatterers (cellular components of the vessel). For each MW, Δ was estimated by numerically solving the optical flow equation (Horn 1986).

RESULTS

Figure 1 presents results for patient 1. A B-mode image is shown in Fig. 1a., whereas Fig.1b gives an illustration of the manual tracing that was performed by a cardiologist with expertise in IVUS imaging to segment the vessel wall. The atherosclerotic plaque was predominant over the left portion of the vessel wall. A “hypo-echoic” artifact is observed at 8 o’clock because the single-element transducer did not sweep the ultrasound beam over a complete 360° angle to image the

cross-section of the vessel. Figure 1c maps the radial strain elastogram, given as Δ_{rr} in eqn 2. The left portion of the plaque (white arrow) was characterized by low radial strain values in the range of 0.2%. The relatively “normal” vessel wall on the right side showed radial strain values in the range of 0.7%. This is explicitly shown in the histogram of the whole vessel (Fig. 1d) where those two distinct regions are pointed out. Figure 1e shows the radial shear ($\Delta_{r\varphi}$) elastogram. It is characterized by a mixture of positive and negative radial shear values inside the plaque area.

A B-mode image of patient 2, along with an illustration of the manual traced segmentation, is shown in Fig. 2a. The atherosclerotic plaque, in this case, was located in the right portion of the vessel wall, whereas a “hypo-echoic” artifact was again delineated around 11 o’clock. Figure 2b maps the radial strain elastogram, in which the plaque was characterized by maximum radial strain values close to 0.3%. The “normal” wall showed radial strain values below 0.1%. It is important to notice that the absolute radial strain and shear values for patient 1, patient 2 and patient 3 should not be compared. For instance, the arterial pressure difference and elapsed time between two successive RF images differed. As an example, the radial strains of 0.7% for patient 1, 0.1% for patient 2 and 0.2% for patient 3 all corresponded to the “normal” portion of the arterial wall. Figure 2c reports the equivalent histogram where those two regions can be identified. Interestingly, this deems that the atherosclerotic plaque was mostly made of a lipid core (high radial strain values). Moreover, Fig. 2d maps the radial shear elastogram. It is worth emphasizing the presence of high radial shear values (around 2.5%) at the interfaces between the “normal” vascular tissue and the soft plaque.

Figure 3a shows a manually segmented B-mode image of patient 3 where the atherosclerotic plaque was predominantly identified in the bottom and in the right portions of the vessel wall. Once again, a “hypo-echoic” artifact is observed around 8 o’clock. Figure 3b maps the radial strain elastogram. As seen, the plaque area presented a very inhomogeneous pattern, where high as well as low radial strain values are observed. The presence of “shadowing” artifacts is observed at 3 and 9 o’clock on the elastogram Δ_{rr} . Some softening artifact is also observed at the most external portion of the vessel wall around 5 o’clock. Is also presented, on Fig. 3c, the radial shear elastogram ($\Delta_{r\varphi}$). It is worth pointing out the following main two features. First, this elastogram shows very high values of radial shear inside the plaque area (up to 6%). Second, the interfaces between the “normal” vascular tissue and the plaque area present a sudden transition from negative to positive radial shear values.

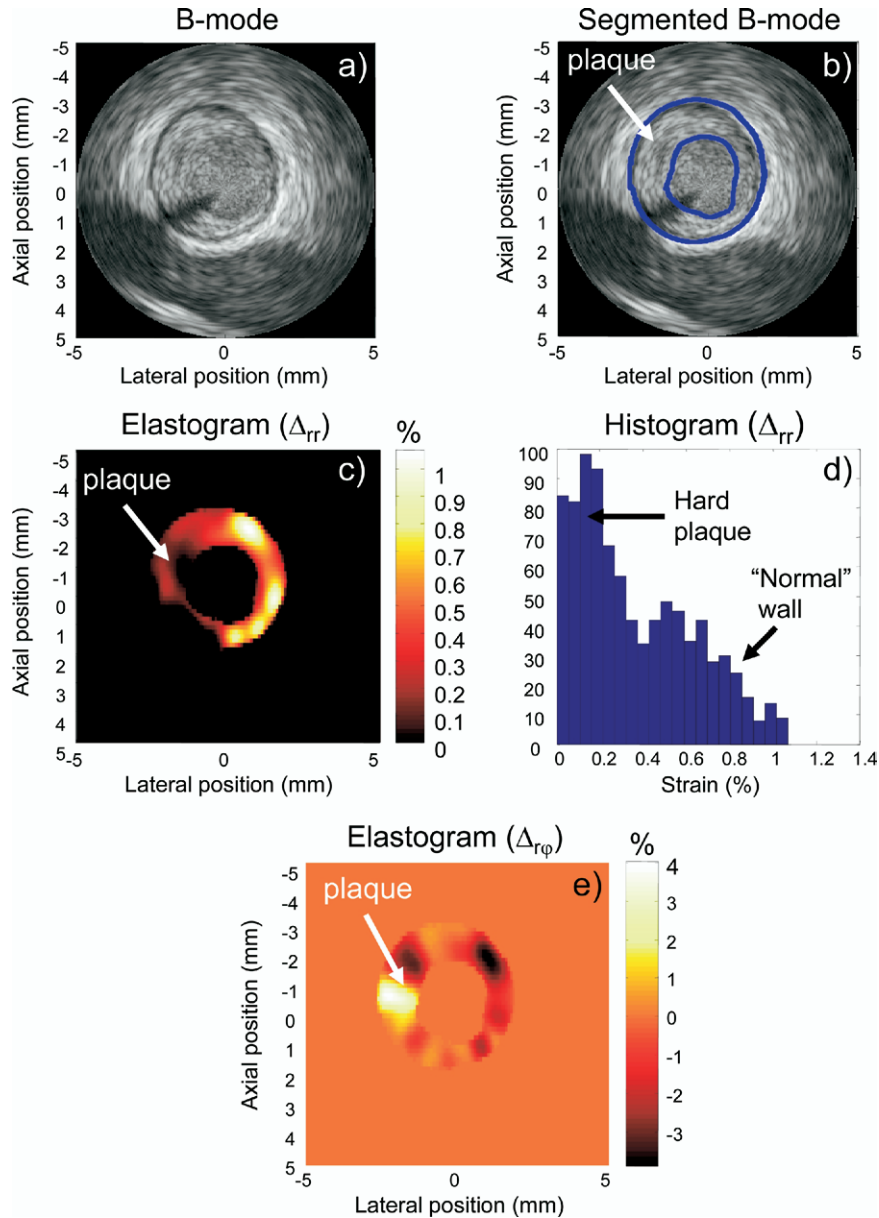


Fig. 1. (a) IVUS image of patient 1; (b) manual tracing of the IVUS image segmentation of the plaque; (c) radial strain elastogram (Δ_{rr} in eqn 2); (d) histogram of the radial strain elastogram; (e) radial shear elastogram ($\Delta_{r\phi}$ in eqn 2).

DISCUSSION

In this article, three patients with atherosclerotic plaques were studied. Ultrasound RF data were recorded during angioplasty, specifically for the purpose of computing elastograms. As it was observed in Figs. 1, 2 and 3, IVUS images mainly give information about atherosclerotic plaque locations, which is insufficient to characterize plaque vulnerability.

About the LE

Complementarily to IVUS images, EVE provides quantitative mechanical parameters to support clinicians

in the diagnosis and in the prognosis of atherosclerosis evolution. Based on the radial strain and shear patterns computed with the LE, it was possible to distinguish different types of plaques, from hard to soft lipid cores. Whereas we can not identify patient 1's plaque stability, plaques of patient 2 and patient 3 may be prone to rupture since lipid cores are known to be vulnerable sites when covered by a thin fibrous cap.

Furthermore, the possibility of assessing quantitative strains could also be a means to provide elastograms of elastic moduli if one knows the instantaneous blood pressure (Baldewsing et al. 2005); this may represent

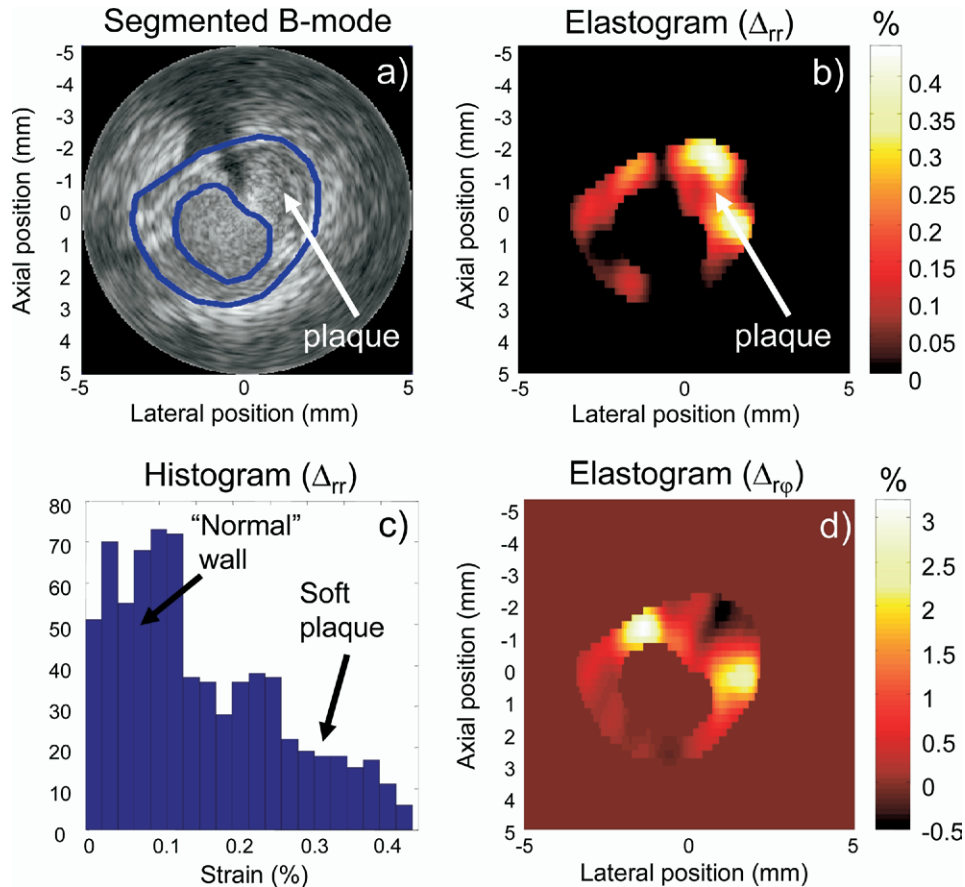


Fig. 2. (a) IVUS image of patient 2 along with the manual tracing that was used for the segmentation; (b) radial strain elastogram (Δ_{rr} in eqn 2); (c) histogram of the radial strain elastogram; (d) radial shear elastogram ($\Delta_{r\phi}$ in eqn 2).

another potential strength of the method, since elastic moduli precisely allow identifying plaque mechanical properties. In addition, for the first time in the elastographic literature, radial shear ($\Delta_{r\phi}$) elastograms were presented. This parameter is important to corroborate radial elastograms and to make postulates about plaque vulnerability. Note that in this study (with a 200 MHz sampling frequency and a measurement window of 200 samples), the worst axial resolution of the elastograms was around 1 mm. This may be a limitation in detecting heterogeneity within small plaques, *i.e.*, with dimensions on the same order of magnitude or less than the measurement window.

About the radial shear elastograms

Regarding patient 1, the $\Delta_{r\phi}$ elastogram (Fig. 1e) showed a mixture of positive and negative radial shear values inside the plaque area. This tends to indicate the heterogeneity of this atherosclerotic plaque even although the radial strain elastogram did not identify any composite material in this zone. The $\Delta_{r\phi}$ elastogram (Fig. 2d), for patient 2, showed high radial shear patterns at the

interfaces between the “normal” vascular tissue and the plaque area. Two main features characterized the $\Delta_{r\phi}$ elastogram (Fig. 3c) for patient 3. Firstly, this elastogram showed high radial shear values inside the plaque area, indicating that a lipid core was part of this atherosclerotic vascular wall. Secondly, the presence of high radial shear values at the interfaces between the normal vessel wall and the plaque area in this elastogram indicates stress concentration sites, which are potential zones prone to vascular tissue rupture.

Furthermore, some “shadowing” artifacts were observed, more specifically in the radial strain elastogram for patient 3 (Fig. 3b); that is due to the presence of negative radial strain values that were set at zero. Negative radial strain values, in this case, resulted from local lost of coherence between RF images in the time-sequence data set. This is likely the case at the interfaces between materials with different mechanical properties due to the complex kinematics (nonrigid rotation, shear, scaling, *etc.*) that are induced. For instance, by comparing radial strain (Δ_{rr}) and radial shear ($\Delta_{r\phi}$) elastograms of Fig. 3, it can be observed that the negative strain

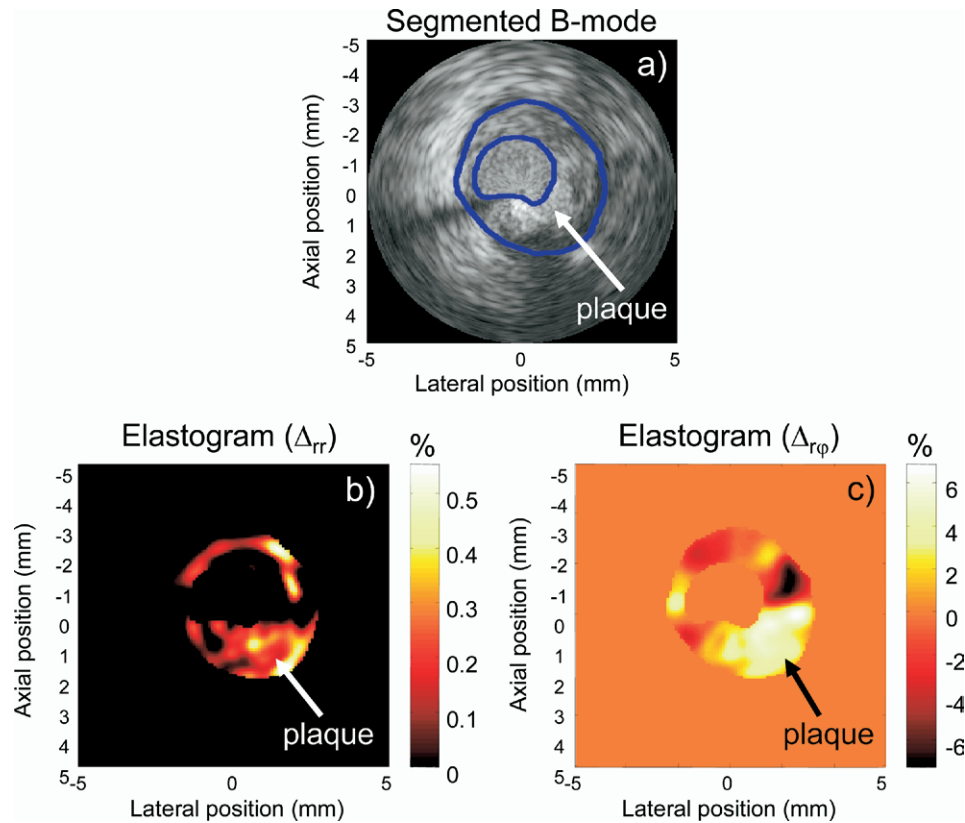


Fig. 3. (a) IVUS image of patient 3 along with the manual tracing that was used for the segmentation; (b) radial strain elastogram (Δ_{rr} in eqn 2); (c) radial shear elastogram ($\Delta_{r\phi}$ in eqn 2).

values were in fact mostly located at the interfaces between the “normal” wall and the plaque area. It is also important to note that the “hypo-echoic” artifact relative to the rotating scanning process may have contributed to the loss of coherence of RF signals. To summarize, the results reported here demonstrate the initial feasibility of the Δ_{rr} and $\Delta_{r\phi}$ elastograms to aid in the prediction of potential sites of plaque rupture and to guide therapy.

About the RF data quality

It is worth emphasizing that data quality was a major concern in this study. Because of a lack of appropriate hardware, the sequences of RF data only contained 5, 7 and 3 images for patient 1, patient 2 and patient 3, respectively. Whereas results reported here are encouraging so far, we do believe that a more appropriate experimental set-up would significantly improve elastograms.

Finally, referring to Figs 1, 2 and 3, the vessel walls were not easily dissociable from the lumen and the surrounding tissues in the RF data. As a consequence, the accuracy of the manual segmentation tracing remains questionable. For example, a specific softening artifact was observed in the radial strain elastogram for patient 3

(Fig. 3b); that was probably due to an over-segmentation of the vascular tissue, since the adventitia is strongly linked to fat tissue (softer) that surrounds the vessel wall.

Discussion summary

In summary, this study has corroborated the clinical relevance of EVE. Whereas no gold standard reference was possible for the purpose of supporting these results, EVE was shown to be a suitable complementary tool to IVUS images. While further experiments are required to validate the robustness of the LE to characterize atherosclerotic plaques, these results give confidence in the potential clinical applications of EVE to characterize plaque vulnerability.

CONCLUSIONS

In this article, *in vivo* applications of the LE on three pathologic human coronary arteries were investigated. The results demonstrated the potential of the method to discriminate between different vascular tissue structures, namely hard and soft materials. More interestingly, it was possible to identify plaques that imbedded lipid cores, which are potentially vulnerable plaques. Addi-

tionally, the first ever *in vivo* radial shear elastograms, with respect to EVE, were reported. Such a characterization parameter, which was provided by the LE, will be used in future studies to determine plaque stability. Indeed, it will support the radial strain elastogram in the identification of atherosclerotic plaques that “shelter” lipid pools; it will also help in the identification of plaque areas subjected to high shear stresses. This can provide important insights for endovascular therapy planning and preoperative lesion assessments, provided that lipid pools and high shear stresses are known to have strong correlations with unstable plaques.

Acknowledgments—This work was supported by grants from the Natural Sciences and Engineering Research Council of Canada (No. 138570-01) and Valorisation-Recherche Québec (structuring group program). Dr Cloutier is recipient of the National Scientist award from the Fonds de la Recherche en Santé du Québec (2004–2009). The salary of Dr Maurice is partially supported by a research scholarship award from the Fonds de la Recherche en Santé du Québec (2006–2008). Dr Cloutier and Dr Maurice are members of the Department of Radiology and Institute of Biomedical Engineering at the University of Montreal.

REFERENCES

- Baldewings RA, Schaar JA, Mastik F, Oomens CWJ, van der Steen AFW. Assessment of vulnerable plaque composition by matching the deformation of a parametric plaque model to measured plaque deformation. *IEEE Trans Med Imaging* 2005;24:514–528.
- Davies JM, Thomas AC. Plaque fissuring: The cause of acute myocardial infarction, sudden ischemic death and crescendo angina. *Br Heart J* 1985;53:363–373.
- Davies MJ, Richardson PD, Woolf N, Katz DR, Mann J. Risk of thrombosis in human atherosclerotic plaques: Role of extracellular lipid, macrophage and smooth muscle cell content. *Br Heart J* 1993;69:377–381.
- de Korte CL, Van der Steen AFW, Céspedes EI, Pasterkamp G, Carlier SG, Mastik F, Schoneveld AH, Serruys PW, Bom N. Characterization of plaque components and vulnerability with intravascular ultrasound elastography. *Phys Med Biol* 2000;45:1465–1475.
- de Korte CL, Siervogel MJ, Mastik F, Strijder C, Schaar JA, Velema E, Pasterkamp G, Serruys PW, van der Steen AFW. Identification of atherosclerotic plaque components with intravascular ultrasound elastography *in vivo*: A Yucatan pig study. *Circulation* 2002;105:1627–1630.
- Falk E. Morphologic features of unstable atherosclerotic plaques underlying acute coronary syndromes. *Am J Cardiol* 1989;63(Suppl. E):114E–120E.
- Falk E. Why do plaques rupture? *Circulation* 1992;86(Suppl. III):30–42.
- Fisher A, Gustin DE, Fayad ZA, Fuster V. Predicting plaque rupture: Enhancing diagnosis and clinical decision-making in coronary artery disease. *Vasc Med* 2000;5:163–172.
- Fuster V, Moreno PR, Fayad ZA, Corti R, Badimon JJ. Atherothrombosis and high-risk plaque: Part I: Evolving concepts. *J Am Coll Cardiol* 2005;46:937–954.
- Fung YC. Biomechanical properties of living tissues. New York: Springer Verlag 2nd ed. 1993;568.
- Horn BKP. Robot vision. New York: McGraw-Hill Company, 1986; 278–298.
- Maurice RL, Ohayon J, Finet G, Cloutier G. Adapting the Lagrangian speckle model estimator for endovascular elastography: Theory and validation with simulated radio-frequency data. *J Acoust Soc Am* 2004a;116:1276–1286.
- Maurice RL, Ohayon J, Frétygn Y, Bertrand M, Soulez G, Cloutier G. Noninvasive vascular elastography: Theoretical framework. *IEEE Trans Med Imaging* 2004b;23:164–180.
- Maurice RL, Brusseau É, Finet G, Cloutier G. On the potential of the Lagrangian speckle model estimator to characterize atherosclerotic plaques in endovascular elastography: *In vitro* experiments using an excised human carotid artery. *Ultrasound Med Biol* 2005a;31:85–91.
- Maurice RL, Daronat M, Ohayon J, Stoyanova É, Foster FS, Cloutier G. Non-invasive high-frequency vascular ultrasound elastography. *Phys Med Biol* 2005b;50:1611–1628.
- Naghavi M, Libby P, Falk E, et al. From vulnerable plaque to vulnerable patient, a call for new definitions and risk assessment strategies: Part I. *Circulation* 2003;108:1664–1672.
- Ohayon J, Teppaz P, Finet G, Rioufol G. *In vivo* prediction of human coronary plaque rupture location using intravascular ultrasound and the finite element method. *Coronary Artery Disease* 2001;12:655–663.
- Zaman AG, Helft G, Worthley SG, Badimon JJ. The role of plaque rupture in coronary artery disease. *Atherosclerosis* 2000;149:251–266.